

Sensitive Determination of Zn^{2+} , Cd^{2+} and Pb^{2+} at Electrochemically Reduced Nanoporous Graphene Oxide/Bismuth Film Electrode

Wang Ren, Ying Zhang*, Minjiao Li

School of Chemistry and Environmental Engineering, Sichuan Provincial Academician (Expert) Workstation, Key Laboratory of Green Catalysis of Higher Education Institutes of Sichuan, Sichuan University of Science and Engineering, Zigong, 643000, P.R. China

*E-mail: zhyrw@163.com

Received: 9 September 2017 / Accepted: 9 December 2017 / Published: 28 December 2017

A sensitive electrochemical sensor was developed for determination of Zn^{2+} , Cd^{2+} and Pb^{2+} based on electrochemically reduced nanoporous graphene oxide (ERNGO) and bismuth film modified electrode. Nanoporous graphene oxide nanosheets were prepared via sono-Fenton reaction of graphene oxide. The structure of NGO was characterized by atom force microscopy and Raman spectrum, and the porosity of NGO nanosheet was verified. The NGO was electrochemically reduced onto glassy carbon electrode surface (ERNGO/GCE), providing huge surface area for loading alloy. By virtue of in situ plated bismuth-film, the Zn^{2+} , Cd^{2+} and Pb^{2+} exhibited sensitive stripping currents and high potential resolution on ERNNGO/GCE via square wave anodic stripping voltammetry (SWASV). Under the optimum experiment conditions, the calibration curves for Zn^{2+} , Cd^{2+} and Pb^{2+} were obtained in the range of 20.0-1000.0 nM, 10.0-1000.0 nM and 10.0-1000.0 nM with the detection limits (S/N=3) of 5.0 nM, 2.0 nM and 0.8 nM, respectively. The proposed sensor also displayed good reproducibility, and was successfully applied to the detection of these metal ions in water samples including tap water and river water.

Keywords: Nanoporous graphene oxide; Bismuth film; Sono-Fenton reaction; Square wave anodic stripping voltammetry; Pb^{2+} ; Cd^{2+}

1. INTRODUCTION

The pollution and harmfulness of heavy metal ions including Cd^{2+} and Pb^{2+} have attracted much attention because of their high toxicity and bioaccumulation [1, 2]. Trace hazardous metal ions intake for long time leads to the accumulation of them in the human body, increasing the injury of human

organs [3]. Therefore, it is worthwhile to develop simple and rapid assay for trace level of Cd^{2+} and Pb^{2+} . Both Zinc deficiency and Zinc overdose are harmful in the human body [4, 5], and thus the quantitative determination of Zn^{2+} level is also essential.

Because of the excellent properties, such as simple preparation, high resolution of stripping signals, insensitivity to dissolved oxygen, easy alloying with many target metals, and wide potential window, the eco-friendly bismuth film electrodes have been extensively used for determination of trace heavy metal ions [6-11]. Combining with bismuth film, various excellent carbon nanomaterials including carbon nanotube [12], fullerene [13], Mesoporous Carbon [14], and graphene oxides (GO) [15-22] were used as supporting material to further improve detection sensitivity of heavy metal ions. Among these nanomaterials, GO has received special interests owing to its high specific surface area, high chemical stability under ambient conditions, low costs and good electrical conductivity [23]. In addition, GO possesses oxygen-containing functional groups including hydroxyl, carbonyl, carboxyl and epoxy group [24], which was endowed with hydrophilic character and more active sites for capturing metal ions. However, carbonyl and carboxyl groups mainly locate at the sheet edges, and monolayer GO sheets often suffer from irreversible aggregation due to the π - π restacking and van der Waals forces in practical applications [25], which decreases the accessible surface area of metal ions.

In order to obtain a kind of stable and swell monolayer GO for capturing more metal ions, hydrophobic aromatic sp^2 -bonded carbon atoms locating in the central of GO should be effectively transformed into carbonyl and carboxyl groups. It was reported that mild ultrasonic treatment of graphite in water facilitated its entire exfoliation and form stable aqueous dispersions with almost 1-nm-thick sheets [20]. Furthermore, the Fenton reaction can attack the carbon atoms connected with the oxygen-containing groups, and C-C bonds of GO were broken subsequently. Therefore, jagged edge and holes were produced on the monolayer GO sheet through Fenton oxidation [26-28].

Herein, taking advantage of ultrasonic exfoliation and Fenton reaction, monolayer nanoporous GO nanosheets (NGO) were obtained via one pot sono-Fenton reaction. The GO was effectively exfoliated into monolayer GO aqueous dispersion by vigorous ultrasonic, and the monolayer GO sheets were adequately oxidized to NGO with abundant oxygen-containing moieties by Fenton reaction in the same vessel. The resultant NGO was employed for preparing the ERNGO-modified glassy carbon electrode (ERNGO/GCE) through drop coating and electrochemical reduction. Combining ERNGO/GCE with bismuth codeposition, a sensitive electrochemical sensor was constructed for determination of Zn^{2+} , Cd^{2+} and Pb^{2+} by using square wave anodic stripping voltammetry (SWASV). Briefly, the ERNGO/GCE was dipped in a mixture of Bi^{3+} and the target metal ions, and then these metal ions could be accumulated and potentiostatic deposited on the surface of ERNGO/GCE. Finally, these metal ions can be selectively detected using SWASV.

2. MATERIALS AND METHODS

2.1 Materials and apparatus

Graphene oxide suspension (0.5 mg mL⁻¹) was obtained from Shanghai Huayi Group Huayuan Chemical Co., Ltd., (Shanghai, China). 30% H_2O_2 and other reagents of analytical reagent grade were purchased from Chengdu Kelong Chemical Reagents Factory (China), and used as received. The

buffer for the assay was 0.1 M acetate buffer saline (ABS) which was prepared by mixing appropriate amounts of CH_3COOH and CH_3COONa . Stock solutions of Bi^{3+} (100.0 mL, 1.0 mM), Fe^{3+} (100.0 mL, 1.0 mM), Zn^{2+} (100.0 mL, 1.0 mM), Cd^{2+} (100.0 mL, 1.0 mM), and Pb^{2+} (100.0 mL, 1.0 mM) were prepared with $\text{Bi}(\text{NO}_3)_3 \cdot 5\text{H}_2\text{O}$, FeCl_3 , $\text{Zn}(\text{CH}_3\text{COO})_2 \cdot 2\text{H}_2\text{O}$, $3\text{Cd}(\text{NO}_3)_2 \cdot 8\text{H}_2\text{O}$ and $\text{Pb}(\text{NO}_3)_2$, respectively. Bi^{3+} , Zn^{2+} , Cd^{2+} , and Pb^{2+} standards with different concentrations were obtained by diluting the stock solutions with acetate buffer. Ultrapure water (18.2 M Ω cm) was used throughout the experiments.

Electrochemical experiments were performed with a CHI660D electrochemical workstation by using a conventional three-electrode cell including a glassy carbon electrode (2 mm in diameter) as the working electrode, a saturated Ag/AgCl reference electrode, and a platinum wire auxiliary electrode. A KQ-250B ultrasonic bath (400 W, Kun Shan Ultrasonic Instruments Co., Ltd., China) was used for the preparation of nanoporous graphene oxides (NGO). The pH values of solutions were measured with a pH meter (PHS-3G, Shanghai Leici Instrument Company, Ltd., China).

2.2 Preparation of NGO suspension and the modified electrode

The Fenton reaction was carried out in a 100 mL flask which was put into ultrasonic bath. In a typical experiment, 2 mL of 0.5 mg/mL graphene oxides (GO) aqueous solution, and 10 μL of 30% H_2O_2 , 200 μL of 1 mM FeCl_3 , and 48 mL ultrapure water were mixed in the flask. The pH of the mixture was adjusted to pH 5.0 with HCl. The mixed solution was sonicated for 24 h (power: 400 W). After the sono-Fenton reaction, the prepared NGO was separated by centrifugation (12000 rpm) for 10 minutes and washed with ultrapure water for three times. Finally, the as-prepared NGO was re-dispersed in 2 mL ultrapure water, and the suspension was stored for further use in a brown glass vessel at 4 °C.

The bare glassy carbon electrode (GCE) was polished with 0.05 μm $\alpha\text{-Al}_2\text{O}_3$ power slurries until a mirror shiny surface, and was sonicated sequentially in HNO_3 (1:1, v/v), alcohol, and double distilled water for 2 min, respectively. After the electrode was thoroughly rinsed with ultrapure water, 20 μL NGO suspension was dropped on the clean GCE surface and allowed to dry at room temperature. Subsequently, bismuth film modified GCE (Bi/GCE), electrochemically reduced NGO modified GCE (ERNGO/GCE), and bismuth film modified ERNGO/GCE (Bi/ERNGO/GCE) were prepared for further testing. The NGO was electrochemically reduced on GCE surface by cyclic voltammograms according to a previous reported method [29] with a little modification: the cyclic voltammograms potential range was choose from 0.0 to -1.5 V for 10 cycles in ABS (scan rate = 20 mV/s, pH 5.0).

2.3 Characterization

Atomic force microscopy (AFM) was used to directly characterize the size and morphology of the GO and NGO. The GO suspension (100 μL) was diluted in 900 μL ultrapure water and sonicated for 1 h as sample 1. The as-prepared NGO suspension (10 μL) was directly diluted in 900 μL ultrapure

water as sample 2. Subsequently, 20 μL of the samples were dropped onto freshly cleaved mica substrates for 10 min. After washing with 1 mL ultrapure water, the samples were dried in air at room temperature. Morphology analysis of NGO was performed with a nanocute/E-SWEEP (Seiko) at relative humidity $<10\%$. Raman spectroscopy (Horiba Jobin Yvon HR800 Raman Microscope System) with 532 nm excitation wavelength was performed to characterize GO (sample 1) and the NGO (sample 2) on the silicon oxide wafer.

2.4 Analytical procedure for Zn^{2+} , Cd^{2+} and Pb^{2+}

The SWASV measurements were performed in 10 mL electrochemical cell, containing 0.1 M acetate buffer (pH 5.0), 1.0 mM Bi^{3+} , and appropriate amounts of Zn^{2+} , Cd^{2+} and Pb^{2+} . The preconcentration was carried out at -1.4 V for 3 min under mild stirring, resulting in codeposition of Bi^{3+} and the target metal ions on the surface of ERNGO/GCE. The stripping voltammograms were recorded between -1.30 V to 0.4 V by applying SWASV without stirring. All experiments were conducted at room temperature (25 ± 2 °C) in air atmosphere.

2.5 Analysis of environmental water samples

Aliquots of the water samples (tap water or river water) were spiked with different concentrations of Zn^{2+} , Cd^{2+} and Pb^{2+} . Other analytical procedures were the same as described above. Tap water was obtained straight from our laboratory. River water was taken from the Fuxi River (Zigong, China). The river water samples were filtered through a 0.22 μm membrane to remove the insoluble impurities.

3. RESULTS AND DISCUSSION

3.1 Characterization of the NGO

The morphology of the GO and as-prepared NGO were characterized by AFM (Fig. 1). The size of GO sheet had a broad distribution of 300 ± 200 nm, and the thickness of GO sheet was about 5 nm (Fig. 1A), indicating GO sheet was comprised of at least five layers [27]. As shown in Fig. 1B, the porous structure in the NGO central plane and jagged edges of NGO basal plane were clearly observed after sono-Fenton process. Thickness of NGO nanosheet was 0.904-0.991 nm (Fig. 1C), indicating that single-layer NGO was successfully exfoliated from each other via the vigorous sono-Fenton reaction. From the images of Fig. 1, the increased surface roughness of NGO was clearly observed. The obviously enhanced surface roughness provides larger surface area than that of smooth exfoliated graphene [15, 18], increasing more active sites and improving accumulation efficiency for the heavy metals.

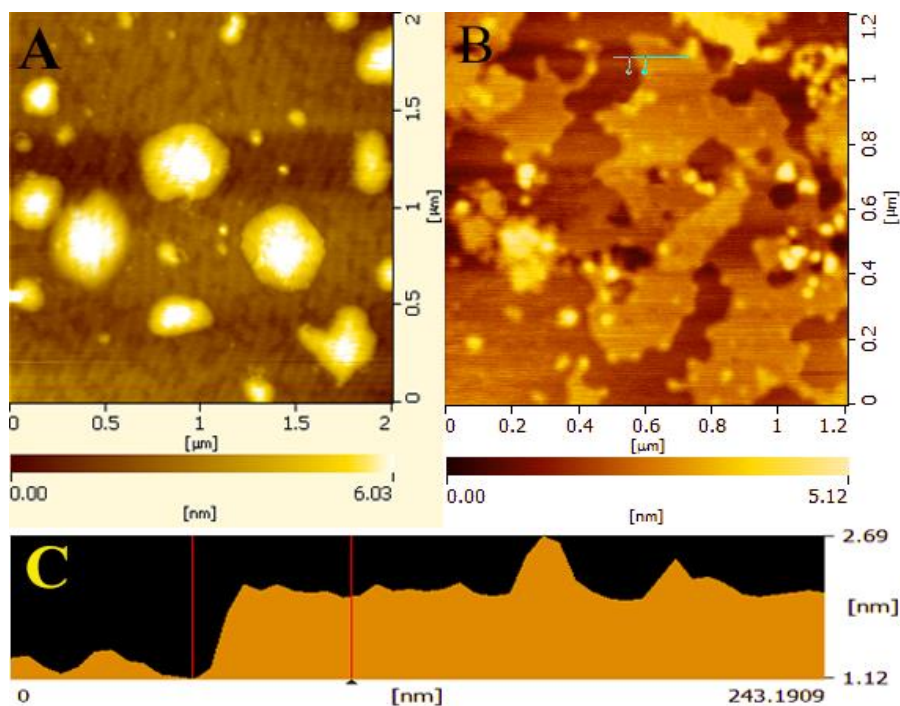


Figure 1. (A) AFM images of GO; (B) AFM images of NGO; (C) Surface roughness of NGO.

As shown in Fig. 2, the D and G bands of GO and NGO were observed in Raman spectra at around 1350 and 1600 cm^{-1} , respectively. Moreover, the intensity ratio of the D band to G band of NGO in Raman spectra was higher than GO, indicating more structural defects of in-plane sp^2 domains and oxygen-containing functional groups in NGO [30-32], which was consistent with AFM results. As we can see from above characterizations, NGO possessed more holes with oxygen functional groups, larger surface area and enhanced roughness than GO.

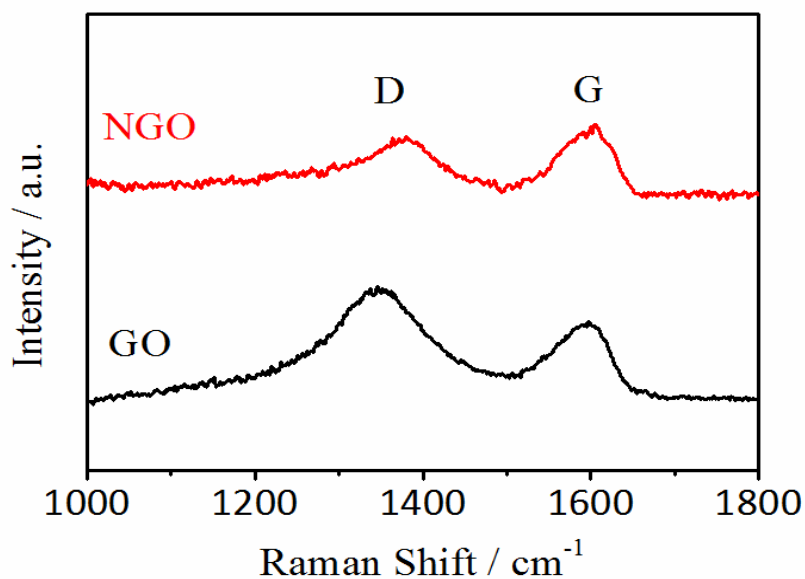


Figure 2. Raman spectrum of GO and NGO with 532 nm excitation wavelength.

3.2 Synergistic effect of NGO and bismuth

The electrochemical performances of different electrodes including ERNGO/GCE, Bi/GCE, and Bi/ERNGO/GCE for simultaneous determination of Zn^{2+} , Cd^{2+} and Pb^{2+} were studied using SWASV. As showed in Fig. 3, the anodic stripping voltammograms of Zn^{2+} (-1.14 V), Cd^{2+} (-0.77 V), and Pb^{2+} (-0.5 V) at ERNGO/GCE (curve a) or Bi/GCE (curve b) appeared three tiny stripping peaks. However, the stripping peak currents of Zn^{2+} , Cd^{2+} and Pb^{2+} at Bi/ERNGO/GCE (curve c) increased dramatically by above 5 folds compared with those at ERNGO/GCE or Bi/GCE. Thus, the abrupt oxidation currents may ascribe to three reasons below: Firstly, nanoporous structures and jagged edges in graphene oxide layers increased surface roughness for permeation and accumulation of heavy metal ions. Secondly, immobilizing NGO on GCE by electrochemically reduced method ensure the stability of the modified electrode. Finally, synergistic effect of bismuth film and ERNGO dramatically advanced the sensitivity. Herein, a new electrochemical sensor was proposed for sensitive detection of Zn^{2+} , Cd^{2+} and Pb^{2+} based on ERNGO/GCE and Bi codeposition.

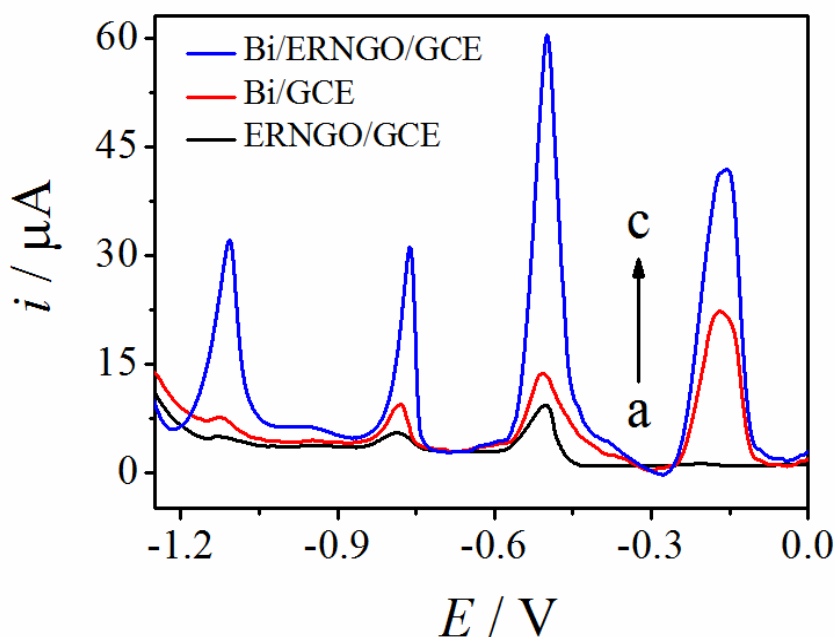


Figure 3. Stripping voltammograms of $1.0 \mu\text{M Zn}^{2+}$, $1.0 \mu\text{M Cd}^{2+}$ and $1.0 \mu\text{M Pb}^{2+}$ at ERNGO/GCE (a), $10.0 \mu\text{M Bi}^{3+}$, $1.0 \mu\text{M Zn}^{2+}$, $1.0 \mu\text{M Cd}^{2+}$ and $1.0 \mu\text{M Pb}^{2+}$ at bare GCE (b) and ERNGO/GCE (c). NGO suspension: $20 \mu\text{L}$; accumulation potential: -1.4 V ; accumulation time: 3 min.

3.3 Optimization of experimental conditions

Considering NGO was the key factor affecting the analytical performance of electrochemical sensor, sono-Fenton reaction time for preparing NGO was studied at first. As depicted in Fig. 4A, the stripping currents of several metal ions increased with increasing sono-Fenton reaction time, and achieves max value at 24 h. Over time, the stripping currents fall down. It was deduced that the amount

of the holes in NGO increased along with prolonged sono-Fenton reaction time [28]. The structure of NGO inhibit the aggregation of GO monolayer via π - π restacking [25]. Thus, the high specific surface NGO modified electrode facilitated permeation and accumulation of metal ions. However, overly longer sono-Fenton reaction time led to smaller NGO fragments or even GO quantum dots [27] which was harder to be immobilized on bare GCE, resulting in the weak stripping signals. Thus, 24h was chosen as the sono-Fenton reaction time for preparing NGO.

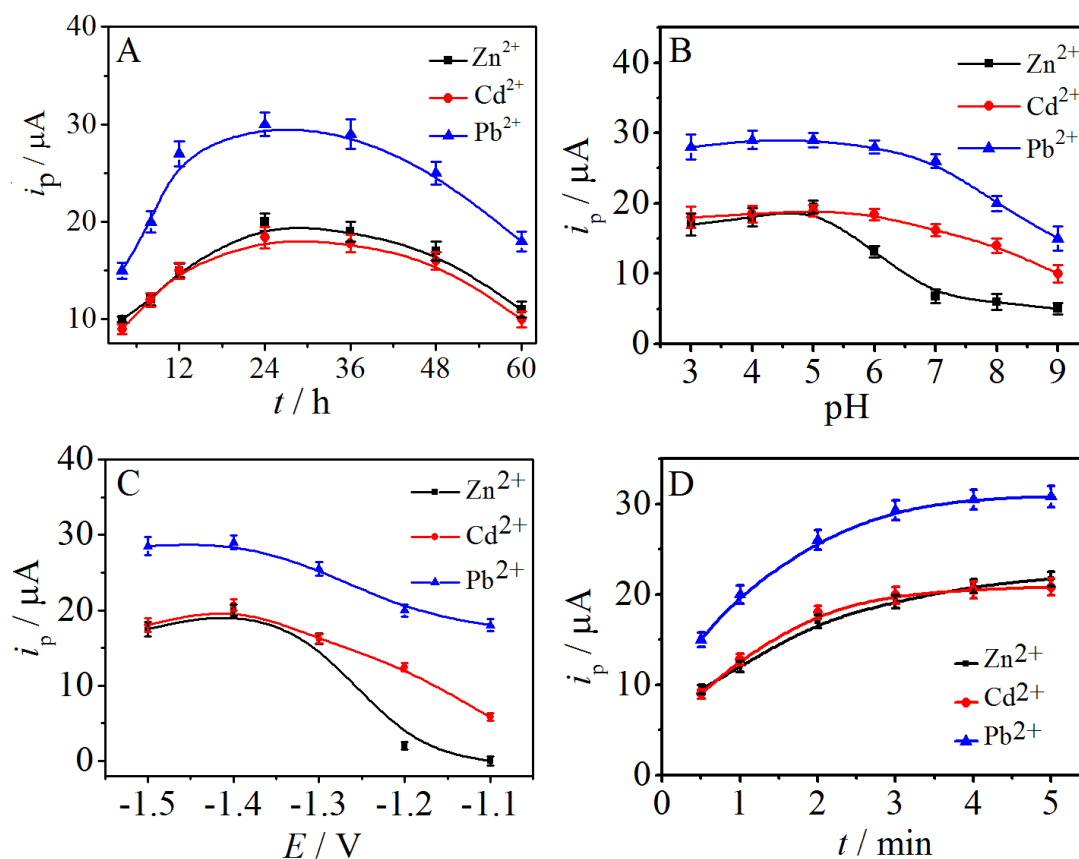


Figure 4. Effect of Fenton reaction time (A), pH of base solution (B), accumulation potential (C), and accumulation time (D) on the stripping peak currents of Zn^{2+} (500.0 nM), Cd^{2+} (500.0 nM) and Pb^{2+} (500.0 nM) at Bi/ERNGO/GCE. Error bar represents the standard deviations of three parallel measurements.

The influences of accumulation conditions including pH value of base solution, accumulation potential and accumulation time were also studied. Different pH values of base solution were investigated, and the results were showed in Fig. 4B. When pH value of base solution changed from 3.0 to 5.0, the stripping peak currents enhanced gradually. When further elevating pH value, the stripping peak currents decreased. So base solution of pH 5.0 was employed for achieving good signal response. The influences of accumulation potential and accumulation time were further investigated. As showed in Fig. 4C, the stripping peak currents of target metal ions were highly variable when changing the accumulation potential from -1.1 V to -1.5 V. Descending accumulation potential until -

1.4 V, the stripping peak currents of Zn^{2+} , Cd^{2+} and Pb^{2+} achieve optimum signal response, which illustrated the more target metal ions were deposited on the surface of ERNGO/GCE. However, when accumulation potential turned negative beyond -1.4 V, the stripping peak currents of target metal ions decreased, because the reduction of H^+ was vigorous, and the interference bubbles hampered the accumulation of metal ions on the modified electrode surface. Thus, the optimized accumulation potential of target metal ions was -1.4 V. The effect of accumulation time was depicted in Fig. 4D. The stripping peak currents of target metal ions increased remarkably along with accumulation time, reaching a plateau at 3 min. Hence, 3 min was chosen as the accumulation time in following experiments.

3.4 Interferences study

Under the optimized conditions, the interference from coexisting metal ions such as Ag^+ , Ni^{2+} , Cu^{2+} , Hg^{2+} , Fe^{2+} , Ca^{2+} , Co^{2+} , Mn^{2+} , Cr^{3+} , and Fe^{3+} was estimated in solution containing target metal ions Zn^{2+} , Cd^{2+} and Pb^{2+} with concentration of 100.0 nM. With a relative error of 5%, no influence was observed when 100 times of Fe^{2+} , Ca^{2+} , Co^{2+} , Mn^{2+} , Fe^{3+} , or Cr^{3+} coexisted. When the concentrations of Ni^{2+} , Hg^{2+} , Cu^{2+} and Ag^+ was beyond 10 folds of target metal ions, there were significant influences on the stripping signals of target metal ions.

In particular, mutual interference between Zn^{2+} , Cd^{2+} and Pb^{2+} was investigated through simultaneous determination of these metal ions at ERNGO/GCE. As shown in Fig. 5A, when the concentration of Cd^{2+} and Pb^{2+} kept constant, the peak current of Zn^{2+} linearly increased with increasing concentration of Zn^{2+} while the other peak currents almost kept invariant. Similarly, only changing the concentration of Cd^{2+} (Fig. 5B) or Pb^{2+} (Fig. 5C), the peak current responses of Cd^{2+} or Pb^{2+} linearly increased while the other two peak currents almost remained the same. The above results indicated that, even adding 100-fold concentration of other cations, there was no mutual interference between Zn^{2+} , Cd^{2+} and Pb^{2+} at ERNGO/GCE.

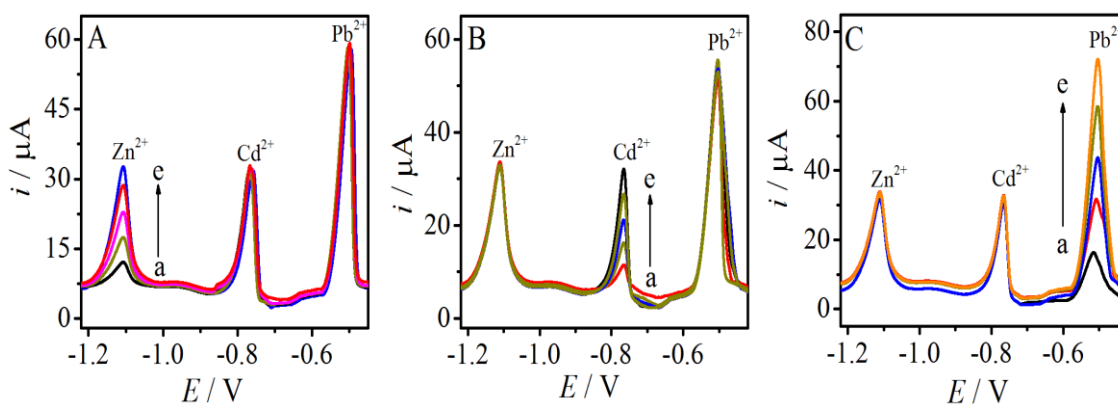


Figure 5. SWASV response of (A) Zn^{2+} (from a to e: 200.0, 400.0, 600.0, 800.0, 1000.0 nM) in the presence of Cd^{2+} (1.0 μM) and Pb^{2+} (1.0 μM); (B) Cd^{2+} (from a to e: 200.0, 400.0, 600.0, 800.0, 1000.0 nM) in the presence of Zn^{2+} (1.0 μM) and Pb^{2+} (1.0 μM); (C) Pb^{2+} (from a to e: 200.0, 500.0, 800.0, 1000.0, 1200.0 nM) in the presence of Zn^{2+} (1.0 μM) and Cd^{2+} (1.0 μM) at Bi/ERNGO/GCE.

3.5 Simultaneous determination of Zn^{2+} , Cd^{2+} and Pb^{2+}

Under the optimized conditions, the resultant sensor exhibited good analytical performance for simultaneous sensing Zn^{2+} , Cd^{2+} and Pb^{2+} in different concentrations (Fig. 6A). As can be seen in Fig. 6B, Fig. 6C, and Fig. 6D, good calibration curves were obtained between the stripping peak currents and the concentrations of corresponding metal ion. The linear ranges of Zn^{2+} , Cd^{2+} and Pb^{2+} , as well as limits of detection, were listed in Table 1. The linear regression equations were $i_p(Zn^{2+}) = 6.2679 + 26.8362C_{Zn^{2+}}$ ($R=0.9994$), $i_p(Cd^{2+}) = 3.8662 + 28.8799C_{Cd^{2+}}$ ($R=0.9991$), and $i_p(Pb^{2+}) = 0.9833 + 57.2166C_{Pb^{2+}}$ ($R=0.9996$), respectively. The detection limits of Zn^{2+} , Cd^{2+} and Pb^{2+} were calculated to be 5.0 nM, 2.0 nM and 0.8 nM, and ($S/N=3$), respectively.

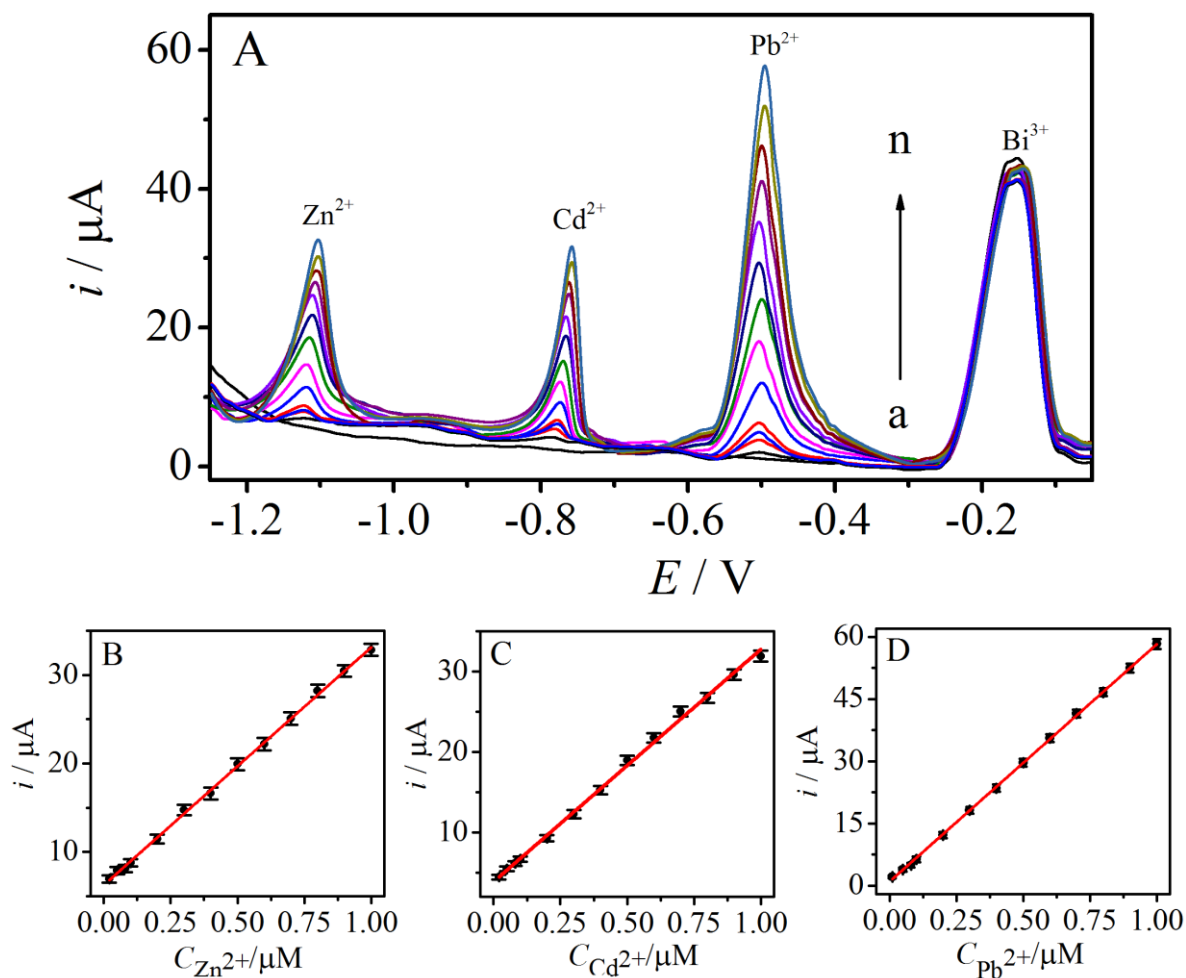


Figure 6. (A) Typical SWASV curves for simultaneous analysis of Zn^{2+} , Cd^{2+} and Pb^{2+} with different concentrations: (a) 0; (b), 20.0 nM (Zn^{2+}), 10.0 nM (Cd^{2+}), and 10.0 nM (Pb^{2+}); (c) 50.0 nM; (d) 80.0 nM; (e) 100.0 nM; (f) 200.0 nM; (g) 300.0 nM; (h) 400.0 nM; (i) 500.0 nM; (j) 600.0 nM; (k) 700.0 nM; (l) 800.0 nM; (m) 900.0 nM; (n) 1000.0 nM at Bi/ERNGO/GCE. Calibration curves for simultaneous determination of (B) Zn^{2+} , (C) Cd^{2+} and (D) Pb^{2+} .

Furthermore, the analytical performance of Bi/ERNGO/GCE for sensing Zn^{2+} , Cd^{2+} and Pb^{2+} was compared with analogous bismuth-based electrode, and the results were listed in Table 1.

Compared to the simple sensors such as CNT [36], Bi-GC [37], SNAC/GCE [39], the proposed sensor remarkably improved both of sensitivity and linear range. The proposed sensor also exhibited an easier preparation and a relatively lower detection limit than those of some reported sensors based on bismuth composite nanomaterials [9, 12, 17-20, 33, 38]. The results indicated that the integration of ERNGO/GCE and bismuth deposition improved the sensitivity for simultaneous determination of Zn^{2+} , Cd^{2+} and Pb^{2+} . Besides, the sensor exhibited excellent analytical stability which may ascribe to immobilizing NGO by electrochemical reduction. The stripping currents of Zn^{2+} , Cd^{2+} and Pb^{2+} only suppressed 7.8, 6.0, and 5.5 % after two hundred times test in 20 days. The reproducibility of the proposed sensor was investigated by analyzing Zn^{2+} , Cd^{2+} and Pb^{2+} standard solution (100.0 nM) for nine replicate determinations. The results showed that the RSD % was calculated to be 4.8%, 5.3% and 4.3% for Zn^{2+} , Cd^{2+} and Pb^{2+} , respectively. The above results demonstrated that the proposed sensor showed high sensitivity and reproducibility for the detection of target heavy metal ions.

Table 1. Comparison of the proposed sensor with previously reported electrochemical sensors for the simultaneous determination of Zn^{2+} , Cd^{2+} and Pb^{2+}

Electrodes	Linear range (nM)			Limit of detection (nM)			Ref.
	Zn^{2+}	Cd^{2+}	Pb^{2+}	Zn^{2+}	Cd^{2+}	Pb^{2+}	
Bi/p-ABSA/GCE	15-1680	9-980	5-630	9.5	5.6	3.9	7
Nafion/Bi/PPF/ Al_2O_3	10-100	10-100	10-100	24	6	3	9
BiOCl/MWNT/GCE	-	45-450	24-240	-	35.6	9.2	12
PANI/OMC/GCE	-	1-120	1-120	-	0.26	0.16	14
GS-Bi/GCE	-	4.5-890	0.5-480	-	3.1	0.2	15
AG-NA/Bi/GCE	76-1530	45-890	24-480	8.7	0.6	0.3	16
ERGO/Bi/SPE	-	9-530	4.8-290	-	4.5	3.9	17
G-Bi/GCE	-	10-85000	10-85000	-	3.0	3.0	18
GTRGO-Bi/Au	-	9-890	4.8-483	-	9	2	19
RGO/Bi/CPE	1530-6116	178-1070	100-580	260	25	2.7	20
Bi/Nafion/RGO/GCE	-	9-800	4.8-435	-	0.7	0.6	21
ERGO-TH-MES/GCE	-	9-357	4.8-200	-	0.9	0.25	22
Nafion/Bi/NMC/GCE	-	90-890	48-480	-	13.3	2.4	33
Bi/Nafion-GO/GCE	-	13-267	2.4-240	-	0.2	0.1	34
MPCS/Cys/GCE	-	500-5000	100-800	-	184	271	35
CNT	2000-8000	1000-4000	500-3000	67	25	12	36
Bi-GC	-	180-890	100-480	-	4.4	2	37
C-Bi/CPE	-	9-890	5-480	-	5.3	2.9	38
SNAC/GCE	-	90-4800	90-5700	-	24.4	5.7	39
Bi/ERNGO/GCE	20-1000	10-1000	10-1000	5.0	2.0	0.8	This work

3.6 Sample analysis

To evaluate the practical application of designed Bi/ERNGO/GCE, several environmental water samples from tap water and Fuxi River water were analyzed. The samples spiked with different concentrations of Zn^{2+} , Cd^{2+} and Pb^{2+} were detected according to the foregoing procedure with five replicates. The recoveries of the target metal ions were in the range of 93.3%–107.8%, and the results

were summarized in Table 2. The results demonstrated that the proposed electrochemical sensor can be successfully applied to determination of Zn^{2+} , Cd^{2+} and Pb^{2+} in real environmental samples.

Table 2. Analysis results of Zn^{2+} , Cd^{2+} and Pb^{2+} in environmental water samples using the proposed electrode

Sample	Analytes	Added (200.0 nM)		Added (500.0 nM)	
		Founded (nM)	Recovery (%)	Founded (nM)	Recovery (%)
Tap water 1	Zn^{2+}	194.4	97.2	478.6	95.5
	Cd^{2+}	190.0	95.0	466.6	93.3
	Pb^{2+}	212.5	106.2	524.0	104.8
Tap water 2	Zn^{2+}	198.0	99.0	498.0	99.6
	Cd^{2+}	206.0	103.0	505.8	101.2
	Pb^{2+}	204.8	102.4	516.0	103.2
River water 1	Zn^{2+}	188.8	94.4	499.6	99.9
	Cd^{2+}	214.2	107.1	520.0	104.0
	Pb^{2+}	215.6	107.8	504.5	100.9
River water 2	Zn^{2+}	198.8	99.4	512.8	102.6
	Cd^{2+}	192.0	96.0	479.0	95.8
	Pb^{2+}	208.0	104.0	486.0	97.2

4. CONCLUSIONS

In conclusion, NGO as an attractive material was facilely prepared using one pot sono-Fenton reaction. Then, combining ERNGO/GCE with bismuth deposition, a new electrochemical sensor was fabricated for the sensitive and simultaneous determination of Zn^{2+} , Cd^{2+} and Pb^{2+} . The resultant sensing platform exhibited high sensitivity and selectivity, and rapid analysis performance. The proposed sensor can be used for the detection of Zn^{2+} , Cd^{2+} and Pb^{2+} in real environmental water samples, showing a great promising for monitoring trace heavy metal ions in practical application.

ACKNOWLEDGEMENTS

This work was financially supported by the Fund Project of Sichuan Provincial Academician (Expert) Workstation (2015YSGZZ03), Sichuan University of Science & Engineering (2016RCL26), the Project of Zigong city (2016XC12), Program of Education Department of Sichuan Province (16ZB0256), and the Opening Project of Key Laboratory of Green Catalysis of Sichuan Institutes of High Education (LYJ1501, LYJ1402).

References

1. J. O. Nriagu, and J. M. Pacyna, *Nature*, 333(1988)134.
2. T. Nawrot, M. Plusquin, J. Hogervorst, H. A. Roels, H. Celis, L. Thijs, J. Vangronsveld, E. V. Hecke, J. A. Staessen, *Lancet Oncol.*, 7 (2006) 119.
3. B. M. Bridgewater and G. Parkin, *J. Am. Chem. Soc.*, 122 (2000) 7140.
4. J. P. Liuzzi, L. A. Lichten, S. Rivera, R. K. Blanchard, T. B. Aydemir, M. D. Knutson, T. Ganz, R. J. Cousins, *P. Natl. Acad. Sci. USA*, 102 (2005) 6843.

5. S. Sazawal, R. E. Black, M. Ramsan, H. M. Chwaya, A. Dutta, U. Dhingra, R. J. Stoltzfus, M. K. Othman, F. M. Kabole, *Lancet.*, 369 (2007) 927.
6. J. Wang, J. Lu, S.B. Hocevar, P.A.M. Farias, B. Ogorevc, *Anal. Chem.*, 72 (2000) 3218.
7. Y. Wu, N. B. Li and H. Q. Luo, *Sens. Actuat. B-Chem.*, 133 (2008) 677.
8. L. Pinto, and S. G. Lemos, *Electroanalysis*, 26 (2014) 299.
9. V. Rehacek, I. Hotovy, M. Vojs, T. Kups, L. Spiess, *Electrochim. Acta*, 63 (2012) 192.
10. J. Wang, *Electroanalysis*, 17 (2005) 1341.
11. I. Švancara, C. Prior, S. B. Hocevar, J. Wang, *Electroanalysis*, 13 (2010) 1405.
12. S. Cerovac, V. Guzsvány, Z. Kónya, A. M. Ashrafi, I. Švancara, S. Rončević, Á. Kukovecz, B. Dalmacija, K. Vytřas, *Talanta*, 134 (2015) 640.
13. N. W. Gothard, T. M. Tritt, J. E. Spowart, *J. Appl. Phys.*, 110 (2011) 023706.
14. L. Tang, J. Chen, G. Zeng, Y. Zhu, Y. Zhang, Y. Zhou, X. Xie, G. Yang, S. Zhang, *Electroanalysis*, 26 (2014) 1.
15. J. Wang, X. Chen, K. Wu, M. Zhang, W. Huang, *Electroanalysis*, 27 (2015) 1.
16. S. Lee, S. Bong, J. Ha, M. Kwak, S. Park, Y. Piao, *Sens. Actuat. B-Chem.*, 215 (2015) 62.
17. J. Ping, Y. Wang, J. Wu, Y. Ying, *Food Chem.*, 151 (2014) 65.
18. M. Wu, H. Li, X. Wang, Q. Wang, P. He, Y. Fang, *Chinese J. Anal. Chem.*, 2 (2013) 278.
19. X. Xuan, M. D. F. Hossain, J. Y. Park, *J. Nanosci. Nanotechnol.* 16 (2016) 11421.
20. P. K. Sahoo, B. Panigrahy, S. Sahoo, A. K. Satpati, D. Li, D. Bahadur, *Biosens. Bioelectron.*, 43 (2013) 293.
21. G. Zhao, H. Wang, G. Liu, Z. Wang, J. Cheng, *Ionics*, 23 (2017) 767
22. Z. Li, L. Chen, F. He, L. Bu, X. Qin, Q. Xie, S. Yao, X. Tu, X. Luo, S. Luo, *Talanta* 122 (2014) 285.
23. A. K. Geim and K. S. Novoselov, *Nat. Mater.*, 6 (2007) 183.
24. A. Lerf, H. He, M. Forster, J. Klinowski, *J. Phys. Chem. B*, 102 (1998) 4477.
25. S. Stankovich, D. A. Dikin, G. H. B. Dommett, K. M. Kohlhaas, E. J. Zimney, E. A. Stach, R. D. Piner, S. T. Nguyen, R. S. Ruoff, *Nature*, 442 (2006) 282.
26. N. A. Zubir, C. Yacou, J. Motuzas, X. Zhang, X. S. Zhao, J. C. D. Costa, *Chem. Commun.*, 51 (2015) 9291.
27. H. Bai, W. Jiang, G. P. Kotchey, W. A. Saidi, B. J. Bythell, J. M. Jarvis, A. G. Marshall, R. A. S. Robinson, *J. Phys. Chem. C*, 118 (2014) 10519.
28. X. Zhou, Y. Zhang, C. Wang, X. Wu, Y. Yang, B. Zheng, H. Wu, S. Guo, J. Zhang, *ACS nano*, 6 (2012) 6592.
29. H. L. Guo, X. F. Wang, Q. Y. Qian, F. B. Wang, and X. H. Xia, *ACS Nano*, 3 (2009) 2653.
30. Y. Li, Y. Z. Liu, W. K. Zhang, C. Y. Guo, C. M. Chen, *Mater. Lett.*, 157 (2015) 273.
31. X. W. Wang, L. Zhou, F. Li, *New Carbon Mater.*, 28 (2013) 408.
32. L. Tang, Y. Wang, Y. Li, H. B. Feng, J. Lu, J. H. Li, *Adv. Funct. Mater.*, 19 (2009) 2782.
33. L. Xiao, H. Xu, S. Zhou, T. Song, H. Wang, S. Lia, W. Gan, Q. Yuan, *Electrochim. Acta*, 143 (2014) 143.
34. J. Li, S. J. Guo, Y. M. Zhai, E. K. Wang, *Anal. Chim. Acta*, 649 (2009) 196.
35. Y. Zhang, J. Zhang, Y. Liu, H. Huang, Z. Kang, *Mater. Res. Bull.*, 47 (2012) 1034.
36. X. Guo, Y. Yun, V. N. Shanov, H. B. Halsall, W. R. Heineman, *Electroanalysis*, 23 (2011) 1252.
37. G. H. Hwang, W. K. Han, J. S. Park, S. G. Kang, *Talanta*, 76 (2008) 301.
38. M. Gich, C. Fernandez-Sanchez, L. C. Cotet, P. Niu, A. Roig, *J. Mater. Chem. A*, 1 (2013) 11410.
39. R. Madhu, K. V. Sankar, S. M. Chen, R. K. Selvan, *RSC Adv.*, 4 (2014) 1225.